Astronomy & Astrophysics manuscript no. master
June 30, 2016

SWEET-Cat update and MOOGme

A new minimization procedure for high quality spectra

D. T. Andreasen[1,2], S. G. Sousa[1], N. C. Santos[1,2], M. Tsantaki[3], G. Teixeira[1], L. Suárez-Andrés[4,5], and A. Mortier[6]

[1] Instituto de Astrofísica e Ciências do Espaço, Universidade do Porto, CAUP, Rua das Estrelas, 4150-762 Porto, Portugal e-mail: daniel.andreasen@astro.up.pt
[2] Departamento de Física e Astronomia, Faculdade de Ciências, Universidade do Porto, Rua Campo Alegre, 4169-007 Porto, Portugal
[3] Instituto de Radioastronomía y Astrofísica, IRyA, UNAM, Campus Morelia, A.P. 3-72, 58089 Michoacán, Mexico
[4] Instituto de Astrofísica de Canarias, E-38205 La Laguna, Tenerife, Spain

[5] Depto. Astrofísica, Universidad de La Laguna (ULL), E-38206 La Laguna, Tenerife, Spain

[6] SUPA, School of Physics and Astronomy, University of St Andrews, St Andrews KY16 9SS, UK

Received ...; accepted ...

ABSTRACT

Aims.
Methods.
Results.

Key words. data reduction: high resolution spectra – stars individual: Arcturus – stars individual: HD010853

1. Introduction

The study of extrasolar planetary systems is an established field of research. To date, over 3200 extrasolar planets have been discovered around solar-type stars[1]. Most of these have been found thanks to the incredible precision achieved in photometric transit and radial velocity methods. Especially the latest announcement from the *Kepler* space mission with 1284 confirmed exoplanets (Morton et al. 2016). The increasing number of exoplanets allow us to do statistical studies of the newfound worlds by analyzing their internal structure, atmospheric composition, with more.

A key aspect to this progress is the characterization of the planet host stars. For instance, precise and accurate stellar radii are critical if we want to measure precise values of the radius of a transiting planet (see e.g. Torres et al. 2012). The determination of the stellar radius is in turn dependent on the quality of the derived stellar parameters such as the effective temperature.

We continue the work of Santos et al. (2013) by deriving parameters in a homogeneous way using the method described in Sousa et al. (2011). This in turn allow us to study planet hosting stars in a homogeneous way and thus new correlations may be found, or higher statistical certainty will be gained on already discovered correlations for planet hosting stars.

2. Data

We use data from different observational runs. The following runs were made particular for this work: 092.C-0695, 093.C-0219, 2014B/020, 094.C-0367, 095.C-0324, and 096.C-0092. Other spectra were found in various archives. We obtain the spectra with the highest possible resolution for a given spectrograph, and in cases there are multiple observations, we include all unless the spectra is close to the saturation limit for a given spectrograph. For multiple spectra, we combine them by after first correcting the radial velocity (RV) and using a sigma clipper to remove cosmic rays. The individual spectra are then combined to a single spectrum for a given star to increase the SNR. This single spectrum is used in the analysis below. We have obtained spectra from UVES (Dekker et al. 2000), FEROS (Kaufer et al. 1999), HARPS (Mayor et al. 2003), FIES (Frandsen & Lindberg 1999), and ESPaDOnS.

3. MOOGme

MOOGme (acronym for MOOG made easy) is a web tool[2] for analyzing spectra. MOOGme is written in Python and works as a wrapper around MOOG (Sneden 1973), and ARES (Sousa et al. 2015) for an all-in-one tool. MOOG is a radiative transfer code under the assumption of local thermodynamic equilibrium (LTE). And ARES is a tool to automatically measure equivalent widths (EW) from a spectrum given a line list. MOOGme has three different modes: Measure EWs with ARES, EW method, and abundances, all described below. We use the Kurucz atmospheric grid from Kurucz (1993).

3.1. EW measurements

EW measurements are essential for the EW method and to obtain abundances. This can be done manually using a tool like IRAF, but often when dealing with a large sample of stars this is

[1] For an updated table we refer to http://www.exoplanet.eu

[2] urlsuper-cool-address-with-MOOGme

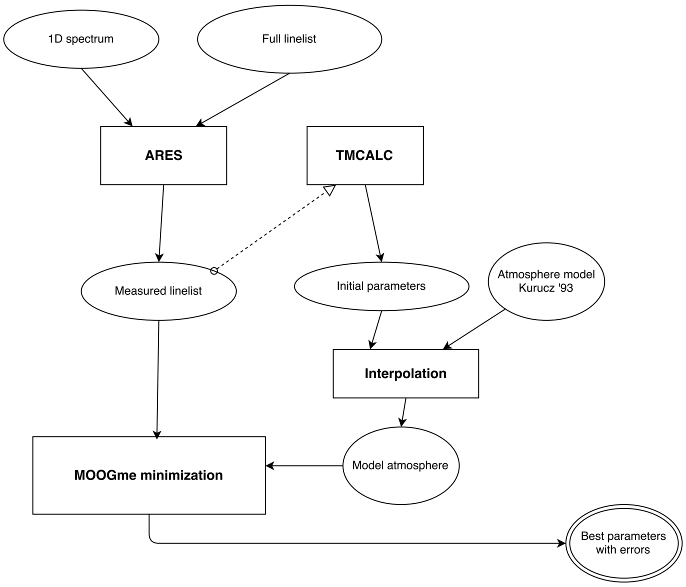

Fig. 1. A general overview over MOOGme from spectrum to parameters.

not a suitable way to deal with the problem. Therefore tools like ARES exists which can measure the EW of spectral lines automatically. To use this mode of MOOGme, it just need a spectrum (format should be 1D fits for ARES to read it) and a line list. For the latter, MOOGme is shipped with some line lists ready to use, in the format suitable for MOOGme. The output will be a line list in the format required for MOOG. The output can be used for either the EW method or the abundance method, both described below.

3.2. EW method

The EW method is a standard method for obtaining parameters from stellar spectra. Here measured EWs are used to calculate abundances using a stellar atmosphere model with a given set of atmospheric parameters, effective temperature (T_{eff}), surface gravity ($\log g$), metallicity ([Fe/H], where iron often is used as a proxy), and the micro turbulence (ξ_{micro}). By removing correlations between the measured abundances (through the measured EWs) and the excitation potential (EP) and reduced EW ($\log(EW/\lambda)$) we can constrain T_{eff} and ξ_{micro}. By obtaining ionization balance between Fe I and Fe II, that is the average abundance of all Fe I lines are equal to the average abundance of all Fe II lines, we constrain $\log g$. Last, we change the input [Fe/H] to match that of the average output [Fe/H]. Hence we have four criteria to minimize simultaneously:

1. The slope between abundance and excitation potential ($a_{\text{EP}} \leq 0.001$).
2. The slope between abundance and reduced EW ($a_{\text{RW}} \leq 0.003$).
3. The difference between the average abundances of Fe I and Fe II ($\Delta\text{Fe} = 0.00$).
4. Input and output metallicity should be equal.

These criteria we denote as indicators for the physical parameters which we are trying to minimize for.

There exists many minimization routines available in Python. Most commonly known are the ones from the SciPy ecosystem[3]. There are some pros and cons with using proprietary minimization routines. Pros are that it is already written, and usually there are good documentation in libraries such as SciPy. Cons in this situation is, that most minimization routines do not work well with vector functions returning another vector:

$$f(\{T_{\text{eff}}, \log g, [Fe/H], \xi_{\text{micro}}\}) = \{a_{\text{EP}}, a_{\text{RW}}, \Delta\text{Fe}, \text{Fe I}\}. \quad (1)$$

A work around is to combine the criteria into one single criteria by e.g. adding them quadratically and minimize that expression instead. Thus we have a vector funtion returning a scalar:

$$f(\{T_{\text{eff}}, \log g, [Fe/H], \xi_{\text{micro}}\}) = \sqrt{a_{\text{EP}}^2 + a_{\text{RW}}^2 + \Delta\text{Fe}^2}. \quad (2)$$

The minimization routines are also not physical in the sense that they are not optimized for the problem. These two cons were incitement for writing a minimization routine optimized for the problem at hand. Here is how it works.

1. Run MOOG once with a user defined initial parameters (default is solar) and calculate a_{EP}, a_{RW}, and ΔFe.
2. Change the atmospheric parameters (T_{eff}, $\log g$, [Fe/H], ξ_{micro}) according to the size of the indicator. A parameter is only changed if it is not fixed.
   - a_{EP}: Indicator for T_{eff}. If this value is positive, then increase T_{eff}.
   - a_{RW}: Same as above but for ξ_{micro}.
   - ΔFe: Same as above but for $\log g$. Positive ΔFe means $\log g$ should be decreased.
   - For [Fe/H] it is changed to the output [Fe/H] in each iteration.
3. If the new parameters have already been used in a previous iteration, then change them slightly. This is done by drawing a random number from a Gaussian distribution with a mean at the current value and a sigma equal to the absolute value of the indicator.
4. Calculate a new atmospheric model by interpolating a grid so we have the requested parameters and run MOOG once again.
5. For each iteration save the parameters used and the quadratic sum of the indicators. If we do not reach convergence, then return the best found parameters.

This whole process is schematically shown in Figure 1 and the minimization routine itself in Figure 2. The stepping follows these simple equations:

$$T_{\text{eff}}+ = \frac{700\,\text{sign}\,(a_{\text{EP}})}{|\log(|a_{\text{EP}}| + 0.0005)|^3} \quad (3)$$

$$\xi_{\text{micro}}+ = \frac{0.05\,\text{sign}\,(a_{\text{RW}})}{|\log(|a_{\text{RW}}| + 0.0005)|^3} \quad (4)$$

$$\log g- = \Delta\text{Fe}\,. \quad (5)$$

The metallicity is corrected at each step so the input metallicity matches that of the output metallicity of the previous iteration. The functional form for changing the parameters were found by trial and error. We are looking for a function that changes rapidly for high indicators, i.e. we are far from the solution, and changes slowly when the indicators have low values. We add a small value (0.0005) for the change in T_{eff} and ξ_{micro}, in order not to take the logarithm of 0. After having a similar function for $\log g$, we see that it could change too rapidly and we will get unphysical requests for parameters with high T_{eff} and low $\log g$. These combinations are not present in the grid we use, and by changing the step in $\log g$ as shown above this problem is solved. The minimum step we allow is $\{1\,\text{K}, 0.01\,\text{dex}, 0.01\,\text{dex}, 0.01\,\text{km/s}\}$ for T_{eff}, $\log g$, [Fe/H], and ξ_{micro}, respectively.

[3] http://scipy.org

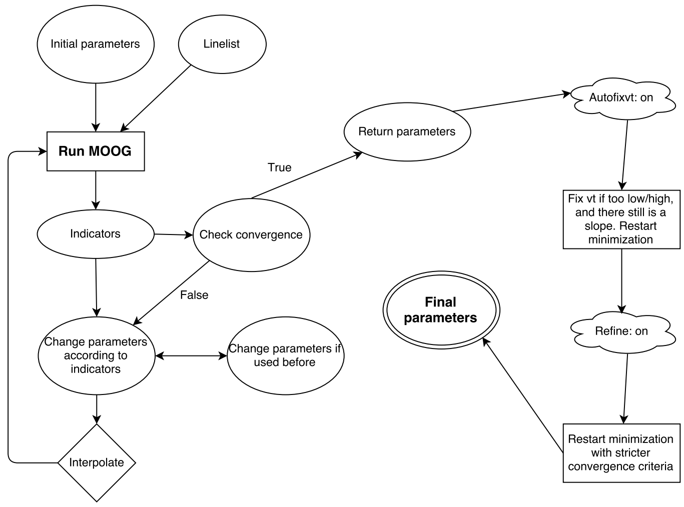

Fig. 2. A schematic overview over the minimization for MOOGme with the EW method.

By using the indicators like this, we can relative fast reach convergence. Typical calculation time for an FGKM dwarf with a high quality spectrum is around 2 min. There are some interdependencies among the indicators. E.g. by changing T_{eff} all indicators will be affected, however the effect is strongest for a_{EP}, so we ignore this interdependence.

3.2.1. Options

It is possible to run the EW method with a set of different options which will be described here.

- *fixteff*: Fix T_{eff}. Same is available for $\log g$ (fixlogg), [Fe/H] (fixfeh), and ξ_{micro} (fixvt).
- *outlier*: Remove outliers after the first run with the minimization routine and restarting the minimization from the previous best parameters. The options are to remove all outliers above 3σ once or iteratively, or remove one outlier above 3σ once or iteratively.
- *autofixvt*: If the minimization routine does not converge and ξ_{micro} is close to 0 or 10 with a significant a_{RW}, then fix ξ_{micro}.
- *refine*: After the minimization is done, run it again from the best found parameters but with more strict criteria. If this option is set, it will always be the last step (after removal of outliers).

If ξ_{micro} is fixed it is changed at each iteration according to an empirical relation. For dwarfs it follows the one presented in Tsantaki et al. (2013) and for giants it follows the one presented in Adibekyan et al. (2015).

We use the line list presented in Sousa et al. (2008). However, this line list does not work well for cool stars. This was fixed in Tsantaki et al. (2013) by removing some lines from Sousa et al. (2008). For stars cooler than 5200 K we rederive the atmospheric parameters after removing lines so the line list resemble that of Tsantaki et al. (2013).

All restarts of the minimization routine is done with initial condition at the last found best parameters.

3.3. Abundance method

With the line list from **?** with XXX different elements it is possible to measure abundances for these elements by combining the ARES mode to measure the EWs and the EW method mode to obtain the atmospheric parameters. The abundances are saved to a table.

3.4. Testing MOOGme

To test the EW method implemented in MOOGme we derive parameters from the 582 sample by Sousa et al. (2011). We use ARES2 to measure the EWs. ARES can give an estimate on the signal to noise ratio (SNR) by analyzing the continuum in given intervals. For solar type stars the following intervals are working well: 5764-5766 Å, 6047-6053 Å, and 6068-6076 Å. From the estimated SNR, ARES can give an estimate on the very important *rejt* parameters (see Sousa et al. 2015, for more information). After measuring the EWs with ARES, we use the MOOGme minimization described in Section 3.2 to determine the stellar atmospheric parameters. The results are presented in Figure 3 which shows T_{eff}, $\log g$, [Fe/H], and ξ_{micro} for MOOGme against those of Sousa et al. (2011).

The sample contains stars with T_{eff} too cold for the line list used. As described in Section 3.2 we should then convert the line list by Sousa et al. (2008) to the line list presented in Tsantaki et al. (2013). However, since this line list was not available when Sousa et al. (2011) derived parameters, we do not make this change in order to make a better test for MOOGme.

The mean of the difference between parameters from Sousa et al. (2011) and those by MOOGme are presented in Table 1.

Table 1. The difference in derived parameters by Sousa et al. (2011) and MOOGme.

Parameter	Mean difference	Mean difference (same line list)
T_{eff}	16 ± 36 K	21 ± 11 K
$\log g$	-0.04 ± 0.07	-0.007 ± 0.009
[Fe/H]	0.03 ± 0.02	0.004 ± 0.009
ξ_{micro}	-0.04 ± 0.14 km/s	0.04 ± 0.02 km/s

We see small offsets that can be due to different versions of MOOG, measured line lists, interpolation of atmosphere grid, and minimization routine. We therefore randomly selected 20 stars with different T_{eff} and used the line lists directly from Sousa et al. (2011) to derive parameters. The results are presented in the last column of Table 1. We note that the $\log gf$ values from the original line lists by Sousa et al. (2011), which used the MOOG 2002 version, were not changed for the 2014 version of MOOG. This might lead to some errors as well. However, the offsets are very small and compatible with the errors on parameters normally obtained from high quality spectra.

3.5. Web interface

NOTE: This section is probably not necessary...

We provide a web interface for MOOGme. In the web interface it is possible to use some of the line list provided with MOOGme to measure EWs of a spectrum (has to be provided by the user). This can be used for all the available MOOGme methods described above.

The web interface can be found at the following link `super-cool-address-with-MOOGme`.

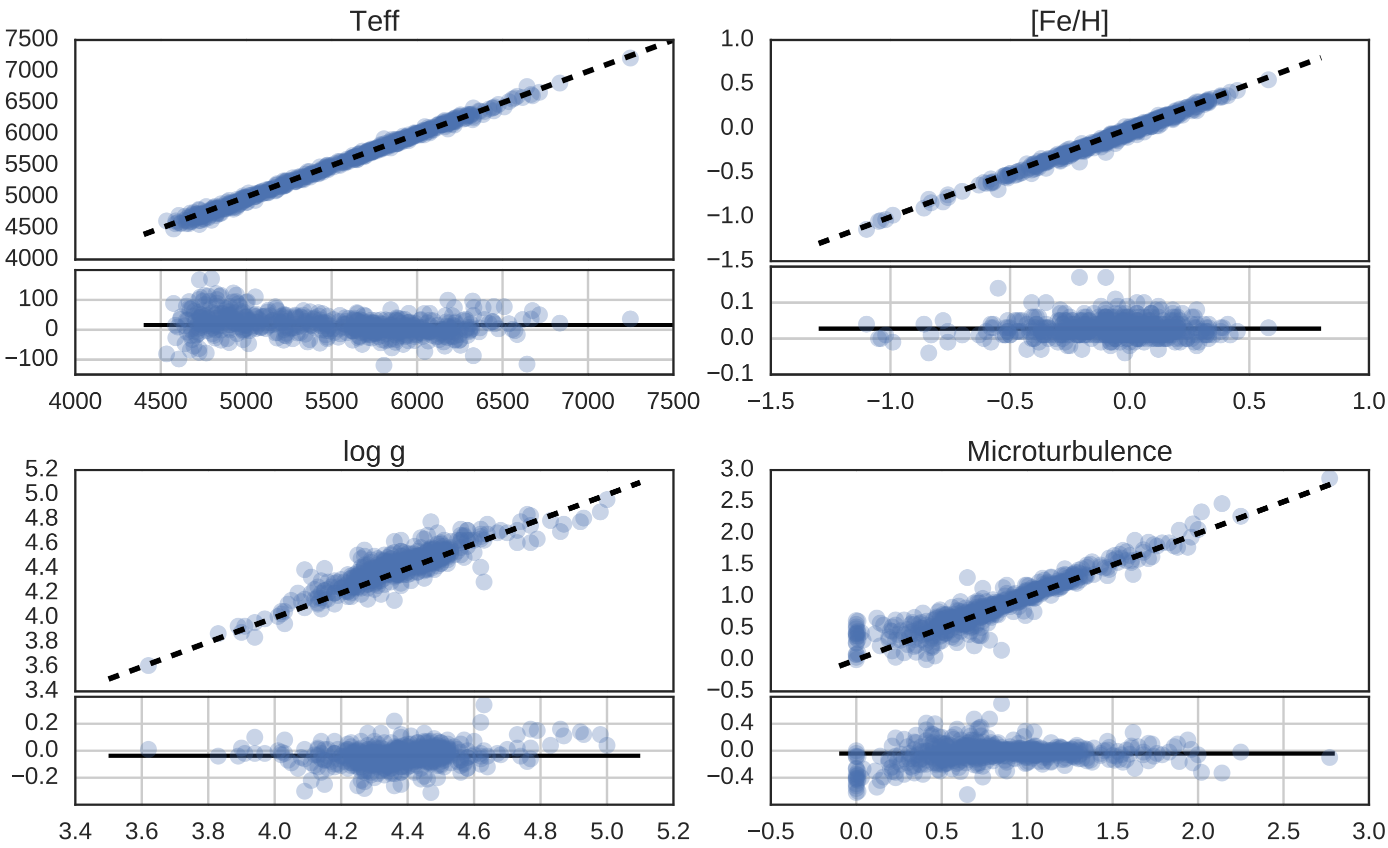

Fig. 3. Stellar atmospheric parameters derived by MOOGme compared to the sample by Sousa et al. (2011).

4. New spectroscopic parameters for 49 planet hosts

Here we present the sample of 50 stars. We were unable to derive parameters for HD77065. This is a spectroscopic binary according to Pourbaix et al. (2004).

The remaining 49 stars are presented in Table 2.

We present a Hertzprung-Russel diagram (HRD) of our sample in Figure 4.

Figure 4 is made with a tool for post processing the results saved to a table by MOOGme. We also use isochrones (Morton 2015) to give an estimate of the age. The mass estimation is based on the relation by Torres et al. (2010). The age estimation is dependent on the mass of the star and the metallicity, which can be seen Figure 5.

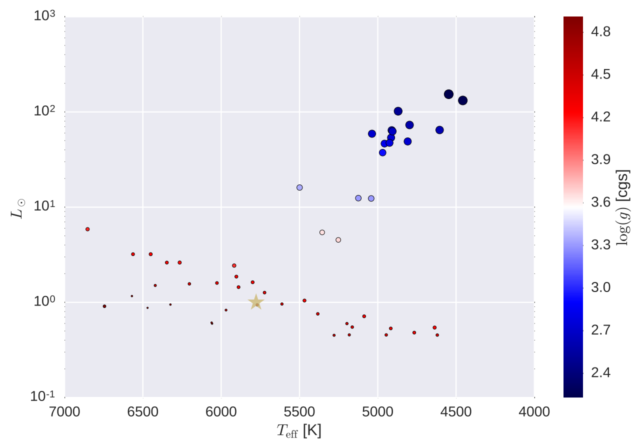

Fig. 4. Hertzprung-Russel diagram of our sample with the Sun as a yellow star. The size of the points represents the $\log g$, with bigger points being smaller $\log g$ (giants), and vice versa. The colour code show the same as the size. Red points are the dwarfs, while blue points are the giants.

5. Conclusion

Acknowledgements. This work was supported by Fundação para a Ciência e a Tecnologia (FCT) through the research grants UID/FIS/04434/2013 and PTDC/FIS-AST/1526/2014. N.C.S., and S.G.S. acknowledge the support from FCT through Investigador FCT contracts of reference IF/00169/2012, and IF/00028/2014, respectively, and POPH/FSE (EC) by FEDER funding through the program "Programa Operacional de Factores de Competitividade - COMPETE". E.D.M. and B.J.A. acknowledge the support from FCT in form of the fellowship SFRH/BPD/76606/2011 and SFRH/BPD/87776/2012, respectively. This work also benefit from the collaboration of a cooperation project FCT/CAPES - 2014/2015 (FCT Proc 4.4.1.00 CAPES). AM received funding from the European Union Seventh Framework Programme (FP7/2007-2013) under grant agreement number 313014 (ETAEARTH). This research has made use of the SIMBAD database operated at CDS, Strasbourg (France).

Table 2. The derived parameters for the 49 stars in our sample.

Star	$T_{\rm eff}$ (K)	$\log g$ (dex)	[Fe/H] (dex)	$\xi_{\rm micro}$ (km/s)	$\xi_{\rm micro}$ fixed?	Program ID
WASP-76	6347 ± 52	4.29 ± 0.08	0.36 ± 0.04	1.73 ± 0.06	no	2014B/020, 094.C-0367
WASP-82	6563 ± 55	4.29 ± 0.10	0.18 ± 0.04	1.93 ± 0.08	no	2014B/020, 094.C-0367
WASP-88	6450 ± 61	4.24 ± 0.06	0.03 ± 0.04	1.79 ± 0.09	no	2014B/020, 095.C-0324
WASP-95	5799 ± 31	4.29 ± 0.05	0.22 ± 0.03	1.18 ± 0.04	no	2014B/020, 095.C-0324
WASP-97	5723 ± 52	4.37 ± 0.07	0.31 ± 0.04	1.03 ± 0.08	no	2014B/020, 094.C-0367
WASP-99	6324 ± 89	4.70 ± 0.11	0.27 ± 0.06	1.83 ± 0.12	no	2014B/020, 094.C-0367
HATS-1	5969 ± 46	4.61 ± 0.06	−0.04 ± 0.04	1.06 ± 0.08	no	092.C-0695
Qatar-2	4637 ± 316	4.23 ± 0.61	0.09 ± 0.17	0.63 ± 0.83	no	092.C-0695
WASP-44	5612 ± 80	4.47 ± 0.30	0.17 ± 0.06	1.32 ± 0.13	no	092.C-0695
HAT-P-46	6421 ± 121	4.53 ± 0.14	0.16 ± 0.09	1.67 ± 0.18	no	093.C-0219
WASP-52	5197 ± 83	4.47 ± 0.30	0.15 ± 0.05	1.16 ± 0.14	no	093.C-0219
WASP-72	6570 ± 85	4.71 ± 0.13	0.15 ± 0.06	2.30 ± 0.15	no	093.C-0219
WASP-75	6203 ± 46	4.42 ± 0.22	0.24 ± 0.03	1.45 ± 0.06	no	093.C-0219
HAT-P-42	5903 ± 66	4.29 ± 0.10	0.34 ± 0.05	1.19 ± 0.08	no	094.C-0367
HATS-5	5383 ± 91	4.40 ± 0.22	0.08 ± 0.06	0.91 ± 0.14	no	094.C-0367
HD 285507	4620 ± 126	4.42 ± 0.61	0.04 ± 0.06	0.74 ± 0.43	no	094.C-0367
HR 228	5042 ± 42	3.30 ± 0.09	0.07 ± 0.03	1.14 ± 0.04	no	094.C-0367
SAND364	4457 ± 104	2.26 ± 0.20	−0.04 ± 0.06	1.60 ± 0.11	no	094.C-0367
GJ 785	5087 ± 48	4.30 ± 0.10	−0.01 ± 0.03	0.69 ± 0.10	no	60.A-9036(A), 072.C-0488(E), 081.C-0842(D),
HD 120084	4969 ± 40	2.94 ± 0.14	0.12 ± 0.03	1.41 ± 0.04	no	14AF14
HD 192263	4946 ± 46	4.43 ± 0.14	−0.05 ± 0.02	0.66 ± 0.12	no	087.C-0012(B), 192.C-0852(A)
HIP 107773	4957 ± 49	2.83 ± 0.09	0.04 ± 0.04	1.49 ± 0.05	no	085.C-0062(A)
HD 219134	4767 ± 70	4.32 ± 0.17	−0.00 ± 0.04	0.59 ± 0.24	no	07bo03
HD 81688	4906 ± 29	2.69 ± 0.06	−0.21 ± 0.02	1.60 ± 0.03	no	14AF14, 53-202
HD 82886	5124 ± 22	3.30 ± 0.05	−0.25 ± 0.02	1.15 ± 0.03	no	14AF14, 53-202
mu Leo	4605 ± 94	2.61 ± 0.26	0.25 ± 0.06	1.64 ± 0.11	no	11AQ78, 05AC23, 06AF22
HD 87883	4917 ± 68	4.34 ± 0.19	0.02 ± 0.03	0.46 ± 0.21	no	14AF14
HIP 11915	5770 ± 14	4.47 ± 0.03	−0.06 ± 0.01	0.95 ± 0.02	no	072.C-0488(E), 089.C-0732(A), 091.C-0034(A)
omi UMa	5499 ± 52	3.36 ± 0.07	−0.01 ± 0.05	1.98 ± 0.06	no	14AF14
11 Com	4911 ± 38	2.68 ± 0.08	−0.20 ± 0.03	1.56 ± 0.04	no	53-202
HD 102272	5037 ± 80	2.72 ± 0.25	−0.52 ± 0.08	0.67 ± 0.12	no	53-202
HD 104985	4809 ± 48	2.73 ± 0.08	−0.26 ± 0.04	1.65 ± 0.05	no	53-202
HD 114762	6061 ± 83	4.70 ± 0.08	−0.78 ± 0.05	0.02 ± 0.26	no	53-202
omi CrB	4915 ± 33	2.74 ± 0.08	−0.14 ± 0.03	1.57 ± 0.04	no	53-202
HD 152581	5355 ± 82	3.65 ± 0.18	−0.39 ± 0.07	0.60 ± 0.15	no	095.C-0324, 53-202
HD 155358	5917 ± 51	4.12 ± 0.08	−0.55 ± 0.04	1.06 ± 0.08	no	40-203
42 Dra	4547 ± 55	2.23 ± 0.10	−0.31 ± 0.03	1.54 ± 0.05	no	49-202
HD 220842	6027 ± 30	4.35 ± 0.05	−0.08 ± 0.03	1.19 ± 0.04	no	44-210
14 And	4797 ± 44	2.58 ± 0.11	−0.23 ± 0.03	1.58 ± 0.04	no	49-202
HD 233604	4925 ± 44	2.79 ± 0.11	−0.15 ± 0.03	1.62 ± 0.05	no	53-202
HD 37124	5468 ± 32	4.28 ± 0.04	−0.43 ± 0.03	0.67 ± 0.07	no	53-202
HD 97658	5182 ± 43	4.50 ± 0.12	−0.29 ± 0.03	0.77 ± 0.11	no	53-202
Kepler-444	5163 ± 40	4.41 ± 0.11	−0.50 ± 0.03	0.78 ± 0.10	no	53-202
WASP-100	6853 ± 209	4.15 ± 0.26	−0.30 ± 0.12	1.87 ± 0.02	yes	2014B/020 094.C-0367
HAT-P-24	6470 ± 181	4.75 ± 0.26	−0.41 ± 0.10	1.40 ± 0.03	yes	092.C-0695
HAT-P-39	6745 ± 236	4.91 ± 0.46	−0.21 ± 0.12	1.53 ± 0.04	yes	094.C-0367
WASP-61	6265 ± 168	4.21 ± 0.21	−0.38 ± 0.11	1.44 ± 0.02	yes	094.C-0367
HD 70573	5889 ± 186	4.32 ± 0.27	−0.42 ± 0.13	1.14 ± 0.01	yes	53-202

References

Adibekyan, V. Z., Benamati, L., Santos, N. C., et al. 2015, MNRAS, 450, 1900

Dekker, H., D'Odorico, S., Kaufer, A., Delabre, B., & Kotzlowski, H. 2000, in Proc. SPIE, Vol. 4008, Optical and IR Telescope Instrumentation and Detectors, ed. M. Iye & A. F. Moorwood, 534–545

Frandsen, S. & Lindberg, B. 1999, in Astrophysics with the NOT, ed. H. Karttunen & V. Piirola, 71

Kaufer, A., Stahl, O., Tubbesing, S., et al. 1999, The Messenger, 95, 8

Kurucz, R. 1993, ATLAS9 Stellar Atmosphere Programs and 2 km/s grid. Kurucz CD-ROM No. 13. Cambridge, Mass.: Smithsonian Astrophysical Observatory, 1993., 13

Mayor, M., Pepe, F., Queloz, D., et al. 2003, The Messenger, 114, 20

Morton, T. D. 2015, isochrones: Stellar model grid package, Astrophysics Source Code Library

Morton, T. D., Bryson, S. T., Coughlin, J. L., et al. 2016, ApJ, 822, 86

Pourbaix, D., Tokovinin, A. A., Batten, A. H., et al. 2004, A&A, 424, 727

Santos, N. C., Sousa, S. G., Mortier, A., et al. 2013, A&A, 556, A150

Sneden, C. A. 1973, PhD thesis, THE UNIVERSITY OF TEXAS AT AUSTIN.

Sousa, S. G., Santos, N. C., Adibekyan, V., Delgado-Mena, E., & Israelian, G. 2015, A&A, 577, A67

Sousa, S. G., Santos, N. C., Israelian, G., Mayor, M., & Udry, S. 2011, A&A, 533, A141

Sousa, S. G., Santos, N. C., Mayor, M., et al. 2008, A&A, 487, 373

Torres, G., Andersen, J., & Giménez, A. 2010, A&A Rev., 18, 67

Torres, G., Fischer, D. A., Sozzetti, A., et al. 2012, ApJ, 757, 161

Tsantaki, M., Sousa, S. G., Adibekyan, V. Z., et al. 2013, A&A, 555, A150

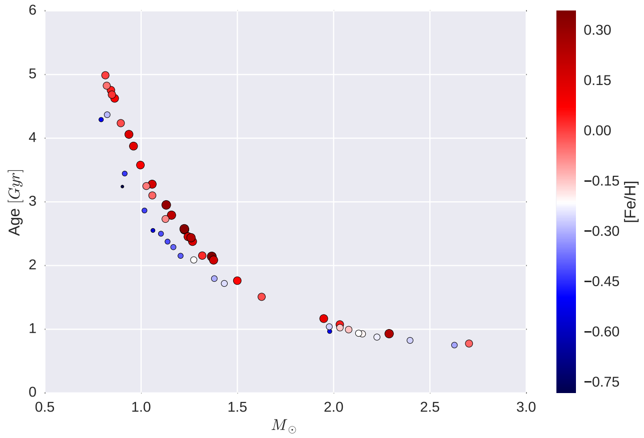

Fig. 5. Age versus mass for our sample, with colours representing the [Fe/H].